Vibration analysis on the mechanisms for hydropower unit rotors based on empirical mode decomposition

XIANGQIAN FU [a,*], HAO XU[a], YATAO LIN[a], ZHIHUI XIAO[a]
[a]*School of Power and Mechanical Engineering, Wuhan University*

According to the coupling faults of mass eccentricity and misalignment, this paper presents a novel vibration analysis method, which employs the nonlinear rotor dynamics with the vibration signal processing scheme based on the Empirical Mode Decomposition (EMD), to understand the vibration mechanism. Such a novel method can decompose the tested signals and compare the simulation results of frequency and normalized energy of intrinsic mode functions (IMF). It is revealed that if the frequency of characteristic IMF is concentrated in the rotating frequency, and the maximum value of IMF is less than 1mm, the rotor is in the state of stable periodic motion; Otherwise, the rotor is in the state of periodic rubbing motion, if frequency of characteristic IMF is concentrated in the rotating frequency and quarter to one-third rotating frequency nearby, the rotor running is in a chaotic motion. The novel method not only provides a new method for vibration signal analysis, but also lays the foundation for fault diagnosis of vibration signals.

(Received August 14, 2013; accepted May 15, 2014)

Keywords: Hydropower unit, Rotor dynamics, EMD, Fault diagnosis, Mode recognition

1. Introduction

The condition monitoring and fault diagnosis of hydropower units is not only related to the power plant safety, but also directly affect the quality of power supply. With the development of technology, the structure of hydraulic turbine is more complex, the individual unit capacity of generator is larger, as well as the mutual influence and mutual coupling between different components of unit is closer, so it leads to more difficulty on monitoring and fault diagnosis. Therefore, the fault diagnosis based on tested signal analysis is one of hot topics, which can ensure the safety, reliability and stability of units, and acquire maximum benefit.

The research about fault diagnosis of hydraulic units mostly focused on the vibration signal analysis, namely, different classification algorithms were applied to identify the fault type of hydraulic unit. For example, the literature [1] used the expert system to diagnose the fault; the literature [2] analyzed the axis orbit based on support vector machine; the literate[3-4] used the neural network as a fault classifier to identify the fault; the literate[5] proposed a new method of vibration signal analysis, namely, fault tree and state diagram; the literate[6-7] used method of rough set to extraction the feature of vibration signal; the literature[8-9] applied a hybrid model to fault diagnosis which combined the neural network with fuzzy logic.

Because of the literate about fault diagnosis of hydraulic turbine less relates to the mechanism of vibration, so the diagnosis results is relatively rough, and the accuracy is hard to guarantee, especially on multi-fault coupling. Therefore, this paper focuses on the multi-fault coupling phenomenon of unbalance, parallel misalignment and angle misalignment. On the one hand, we construct the simulation model based on rotor dynamics to simulate the orbit of hydraulic turbine rotor; On the other hand, we employ the Empirical Mode Decomposition (EMD) method to extract the features of tested signal and simulation signal, and study the relationship between the vibration characteristics and inherent fault mechanism, and then rich connotation of intelligent diagnosis method, achieve the optimal diagnosis of hydroelectric generating units. The research promotes the implementation and development of on-line monitoring and fault diagnosis of hydroelectric generating unit, so it has high scientific significance and engineering application value.

There are many classification and discrimination algorithms which is used to characterize the vibration signal, such as Fourier transform, wavelet/wavelet packet transform and the Hilbert-Huang transform (HHT). Comparing with other classification methods, a series of intrinsic mode function (IMF) of vibration signals is decomposed by the method of empirical mode decomposition(EMD) in the HHT, and the instantaneous frequency of each IMF is obtain by Hilbert transform. The advantage of HHT is able to acquire higher resolution in time domain and frequency domain, so it is suitable for non-stationary and nonlinear signal. For example, Feldman[10] researched the relationship between the mechanical vibration mode and IMF; Yang classify the characteristics of linear multi-degree-freedom structures successfully by the method of HHT.

1.1 Process of empirical mode decomposition

(1)The upper envelope v_1(t) and lower envelope v_2(t) are fitted by the maxima and minima of vibration signal s(t), and *m(t)* is defined as

$$m(t)=\frac{1}{2}[v_1(t)+v_2(t)] \tag{1}$$

and *h(t)* is defined as

$$h(t)=s(t)-m \tag{2}$$

Ideally, if h(t) is an IMF, denoted as $C_1(t)$, which must satisfy the following definition: (1) the number of extra and the number of zero-crossings must either equal or differ at most by one in s(t); (2) At any point, the mean value of the upper envelope and lower envelope is zero.

(3) If h(t) is not an IMF, h(t) is treated as the original signal and repeat (1) up to h(t) becomes an IMF, then it is designated as:

$$C_1(t)=h(t) \tag{3}$$

Separating $C_1(t)$ from s(t), we get

$$R_1(t)=s(t)-C_1(t) \tag{4}$$

where *r1*(t) is treated as the new original signal, and by repeating the above processes, the second IMF component $C_2(t)$ of s(t) could be obtained. Let us repeat the process as described above n times. The n-IMFs of s(t) can be acquired.

The decomposition process can be stopped when $R_n(t)$ becomes a monotonic function from, which on more IMF can be extracted. If ignoring the value of $R_n(t)$, we finally obtain

$$s(t)=\sum_{j=1}^{N}C_j(t) \tag{5}.$$

1.2 The marginal spectrum by Hilbert transform

By Hilbert transform, the analytical signals of each IMF component is defined as:

$$z_j(t)=C_j(t)+i\tilde{C}_j(t)=a_j(t)e^{i\phi_j(t)}=a_j(t)e^{i2\pi\int f_j(t)dt}$$

where $\tilde{C}_j(t)$ is treated as the transform signal of $C_j(t)$,namely, $\tilde{C}_j(t)=\frac{1}{\pi}\int_{-\infty}^{\infty}\frac{C_j(\tau)}{t-\tau}d\tau$, and $a_j(t)$ 、 $\phi_j(t)$ are treated as time-varying amplitude and phase respectively, and $f_j(t)$ is represented as the signal instantaneous frequency, namely $f_j(t)=\frac{d\phi_j(t)}{dt}$.

The real part of formula (4) is as follow

$$C_j(t)=\mathrm{Re}(z_j(t))=\mathrm{Re}(a_j(t)e^{i2\pi\int f_j(t)dt})$$

where the time signal $C_j(t)$ is transform into the function of time t and frequency f. Therefore, the signal s(t) can be transformed into a function of time and frequency i.e.:

$$s(t)=H(f,t)=\mathrm{Re}\sum_{j=1}^{N}a_j(t)e^{i2\pi\int f_j(t)dt} \tag{6}$$

The function of frequency and amplitude of signal by integration of formula (6), which is known as Hilbert marginal spectrum:

$$h(f)=\int_0^T H(f,t)dt \tag{7}$$

The Hilbert marginal spectrum energy of each frequency band could be extracted by formula (8):

$$bp=\sum_{j=f_1}^{f_2}v_j^2/n \tag{8}$$

where v_j is treated as marginal spectrum value of each instantaneous frequency, f_1 、 f_2 is represented as minimum and maximum of frequency band; n is expressed as the number of data point within the frequency band.

2. Dynamic analysis on hydraulic generator rotors with coupling faults based on rotor dynamics

2.1 Model of rotor dynamics

Since the unit rotors vibration induced by oil film oscillation was firstly investigated in the early nineteen twenties [12], the dynamic behaviors of hydraulic unit rotors have been researched for decades and some progress has made. For example, Wan [13-14] established the mathematical model to simulate the oil film oscillation by nonlinear dynamics, through comparing the axis orbit, power spectrum and Poincare map to analyze the bifurcation phenomena of rotors. Gwo-Chung [15] has studied the vibration phenomena of hydraulic turbines which have different number of blades to analyz the dynamic characteristics of the rotors.

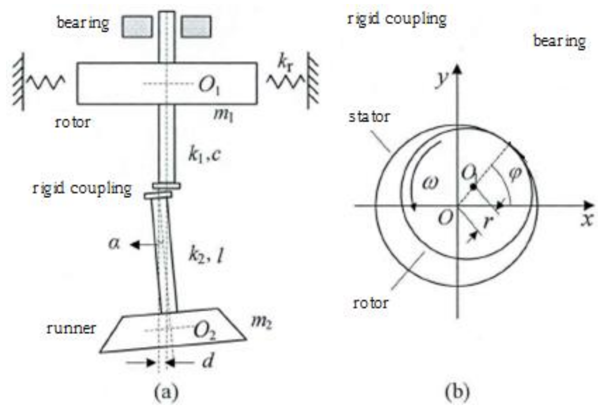

Fig. 1. Simplified model of hydropower unit rotor system.

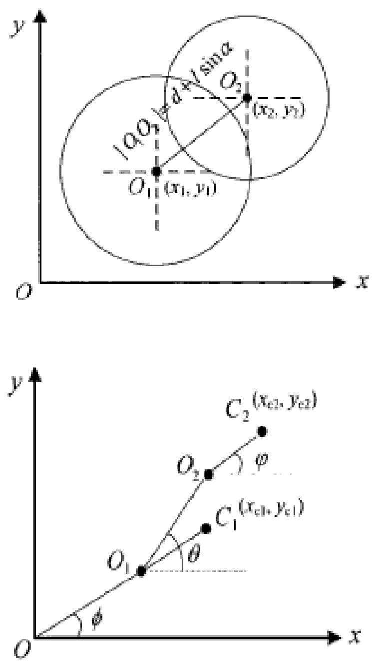

Fig. 2. Schematic diagram of rotor moving with coupling faults.

The simplified model of hydraulic units, including a turbine, a generator, and a shaft with two rotor and one bearing, is shown in fig.1. Various faults types, such as unbalance, misalignment and rubbing, were coupled by this model. In Fig. 1, O is treated as the design geometric center of unit, o_1 (x_1,y_1) and o_2 (x_2,y_2) are represented the initial state of geometric center of generator rotor and turbine rotor respectively. m_1 and e_1 are represented the mass and eccentricity of generator, as well as m_2 and e_2 are represented similar meaning of turbine. In Fig. 2, c_1 (x_{c1},y_{c1}) and c_2 (x_{c2},y_{c2}) are represented the equivalent mass center of generator rotor and turbine rotor respectively.

Dynamic behaviors of hydraulic unit with coupling faults are not only considered the impact of unbalance and misalignment, but also needed to consider the rubbing force and damping force. So the rubbing force can be defined as:

$$\begin{Bmatrix} F_x \\ F_y \end{Bmatrix} = -H(r-\delta)\frac{(r-\delta)k_r}{r}\begin{bmatrix} 1 & -\mu \\ \mu & 1 \end{bmatrix}\begin{Bmatrix} x_1 \\ y_1 \end{Bmatrix} \tag{9}$$

where F_x、F_y are represented as the rubbing force with X direction and Y direction, r is treated as the axis orbit, δ is treated as the gap between the stators and rotors of unit, and $H(r-\delta)$ is treated as switching fuction, namely:

$$\begin{cases} H(r-\delta)=0 & r<\delta \\ H(r-\delta)=1 & r\geq\delta \end{cases} \tag{10}$$

If the damping coefficients with X direction and Y direction have the same value c, the force on the generator rotor can be defined as follow without considering other interferences:

$$\begin{cases} Q_x = -c\dot{x}_1 + F_x \\ Q_y = -c\dot{y}_1 + F_y \end{cases} \tag{11}$$

And the rotor moving energy (T) is mainly composed of translational energy(T_G) and rotational energy(T_r):

$$T_G = \frac{1}{2}m_1 v_{c1}^2 + \frac{1}{2}m_2 v_{c2}^2 = \frac{1}{2}m_1(\dot{x}_{c1}^2+\dot{y}_{c1}^2) + \frac{1}{2}m_2(\dot{x}_{c2}^2+\dot{y}_{c2}^2) \tag{12}$$

where v_{c1}、v_{c2} are represented the linear velocity of generator and turbine respectively, and $\dot{\chi}$ is treated as the time derivative of χ.

At the initial state, the total potential energy of the rotor system can be expressed as:

$$U = \frac{1}{2}k_1|oo_1|^2 + \frac{1}{2}k_2|oo_2|^2 = \frac{1}{2}k_1(x_1^2+y_1^2) + \frac{1}{2}k_2(x_2^2+y_2^2) \tag{13}$$

The dynamics differential equations of hydraulic unit with coupling faults could be obtained by Simultaneous equations (9-13):

$$[M]\ddot{Z} + [C]\dot{z} + Kz = F \tag{14}$$

namely：

$$\begin{bmatrix} m_1+m_2 & 0 \\ 0 & m_1+m_2 \end{bmatrix}\begin{bmatrix} \ddot{x} \\ \ddot{y} \end{bmatrix} + \begin{bmatrix} c & 0 \\ 0 & c \end{bmatrix}\begin{bmatrix} \dot{x} \\ \dot{y} \end{bmatrix} + \begin{bmatrix} k_1+k_2 & 0 \\ 0 & k_1+k_2 \end{bmatrix}\begin{bmatrix} x \\ y \end{bmatrix}$$
$$= \begin{bmatrix} m_1e_1\omega^2\cos\phi + m_2e_2\omega^2\cos\alpha\cos\varphi + m_2(d-l\sin\alpha)\omega^2\cos\theta - k(d-l\sin\alpha)\cos\theta + F_x \\ m_1e_1\omega^2\sin\phi + m_2e_2\omega^2\cos\alpha\sin\varphi + m_2(d-l\sin\alpha)\omega^2\sin\theta - k(d-l\sin\alpha)\sin\theta + F_y \end{bmatrix} \tag{15}$$

2.2 Case analysis

The parameter values of simulation model are same as the experiment test bench, the equivalent parameters are as follows :m_1=5.0kg,m_2=5.2kg,c=2100N*s/m, k_1=2.5*10^6N/m, k_2=2.5*10^6N/m, k_r=2.5*10^7N/m, l=0.5m,e_1=0.05mm,e_2=0 mm, δ =1mm, μ =0.01.

If the rotation rate changes form 0 rad/s to 50 rad/s, the model is solved by the Runge-Kutta model, and the results of generator rotor vibration bifurcation diagram are shown in fig. 3.

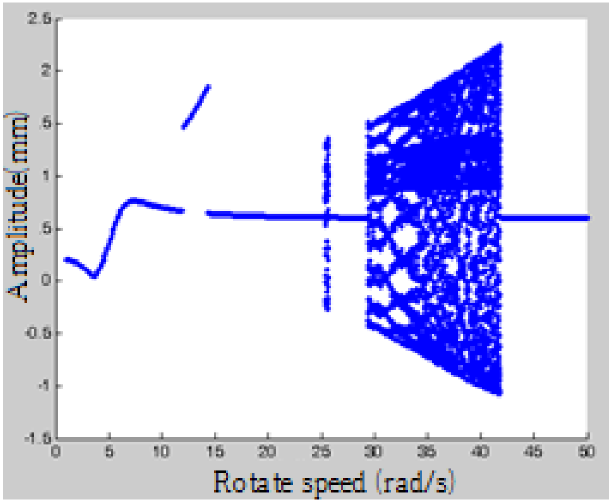

Fig. 3. The vibration bifurcation diagram of generator rotor.

With the increasing of rotation rate, the vibration type can be classified into stable periodic motion, periodic rubbing motion and complicated chaotic motion. When $\omega \in [1,12]$ $\omega \in [14,25]$ $\omega \in [26,29]$ and $\omega \in [42,50]$, the unit is in a stable state and the range of maximum rotor vibration within [0 0.08]mm; when $\omega \in [12,14]$, the maximum rotor vibration is exceeded the bearing clearance, which induces the periodic rubbing phenomenon strongly, so it means the rotor is in periodic rubbing motion. When $\omega \in [25,26]$ and $\omega \in [29,42]$, the operation of rotor is extremely unstable and the rubbing is irregular, so the rotor is in chaotic motion.

3. Experiments

The hydraulic unit vibration test bench in Fig. 4, is a simplification of hydraulic generator unit, which is used to simulate the dynamic features of rotor with coupling faults, such as eccentricity, misalignment and rubbing. And because of small mass and high rigidity of rotor, the influence of rotor gravity is ignored. The test bench is mainly composed of a generator rotor, turbine rotor and shaft, the eccentricity of generator rotor and turbine rotor is controlled by changing the mass of screws in rotor, and the misalignment faults is made by the customized rotor which keep the generator rotor and turbine rotor in misalignment state.

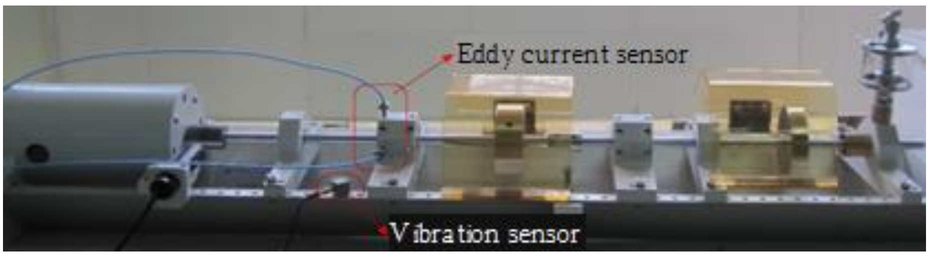

Fig. 4. Hydraulic unit vibration test bench.

The aim of experiment is to verify the credibility of numerical simulation based on analyzing the features of rotor motion, and then it could be provided a foundation for hydraulic generator rotor vibration research with coupling faults by using EMD method. Therefore, the vibration experiment is done with the rotation rate of 5rad/s, 12rad/s and 30rad/s.

4. Research on vibration mechanism of hydropower unit based on EMD

According to the vibration tested signal and corresponding simulation signal under different rotation rate, HHT method is used to acquire the time-frequency characteristics of signal which is shown in Figs. 5-7. By analyzing Figs. 5-7, the generator rotor motion is classified into three type: when the rotation rote are 5rad/s and 12rad/s, the frequency of tested signal is mainly concentrated in the rotating frequency, but the maximum vibration amplitudes of them are different, the former is less than 1mm so the motion of rotor is belong to stable periodic motion, contrarily, the latter is more than 1 mm so the motion of rotor is belong to periodic rubbing motion. At the rotation rate of 30 rad/s, the frequency of tested signal is concentrated in the rotating frequency and quarter to one-third of rotating frequency, and the maximum vibration amplitudes is more than 1mm, so the motion is belong to chaotic motion.

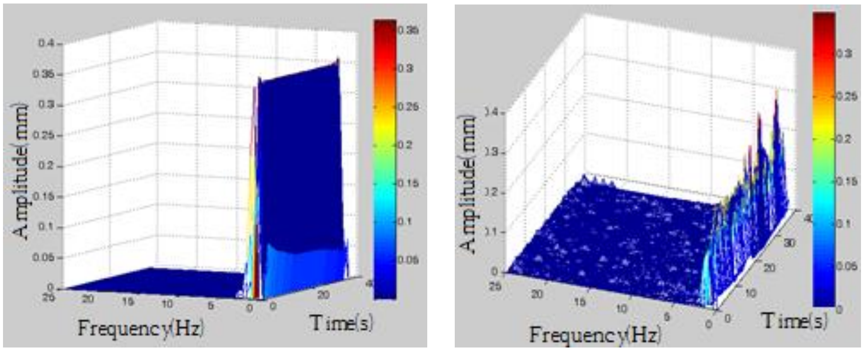

(a) *frequency of simulation signal* (b) *frequency of tested signal*

Fig. 5. Frequency of simulation signal and tested signal at theω=5rad/s.

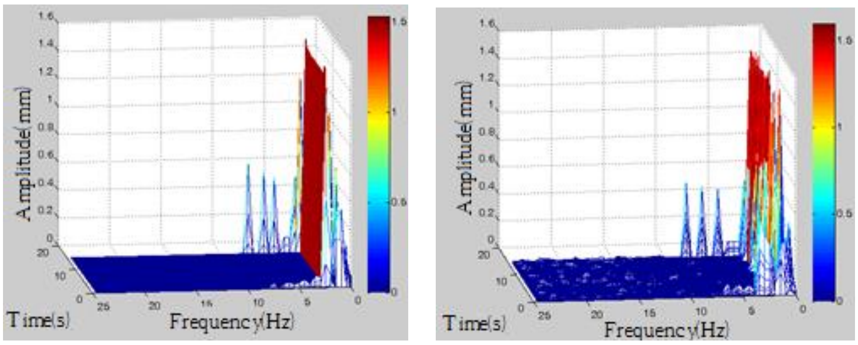

(a) *frequency of simulation signal* (b) *frequency of tested signal*

Fig. 6. Frequency of simulation signal and tested signal at theω=12rad/s.

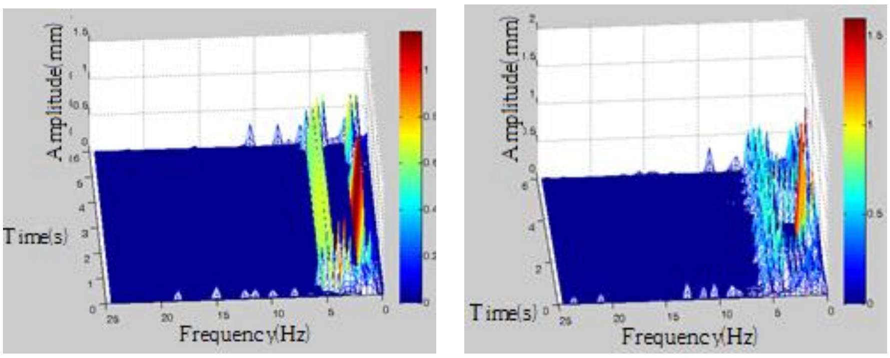

(a) *frequency of simulation signal* (b) *frequency of tested signal*

Fig. 7. Frequency of simulation signal and tested signal at theω=30rad/s.

In Figs. 5-7, with the increase of time, the vibration frequency and vibration amplitude of simulation signals are almost little change, while in the time-frequency analysis of tested signal, the corresponding parameters has obvious changes. The diversity is not only due to the noise signal in the testing process, but also due to the simulation error because the simulation model is simplified from the actual.

The tested signal and simulation signal at rotation rate of 5rad/s are decomposed into IMFs by the method of

EMD , and then we calculate the normalized energy value of each IMFs by improved formula (8), and the results is shown in Table 1. Fig. 8 shows the result of decomposition, the simulation signal is decomposed into four IMFs. And frequency of the first IMF is similar as the simulation signal which is concentrated in the rotating frequency, and the normalized energy of this IMF is 0.84, so this IMF is best represented the features of simulation signal, and physical meaning of this IMF is that the rotor motion is on state of stable periodic motion. Accordingly, the results of tested signal are shown in Fig. 9. The signal is decomposed into 10 IMFs, and the frequency of each IMF has signification difference, especially high frequency decompositions and low frequency decompositions. Wherein, the frequency of fifth IMFs and sixth IMFs focus on rotating frequency nearby, and the normalized energy is 0.65, so the two IMFs is employed to represents the intrinsic physical meaning of measured signal, namely, in spite of unbalance and misalignment force, because the effect of coupling faults on the rotor is weak, the rotor running is in a stable periodic motion.

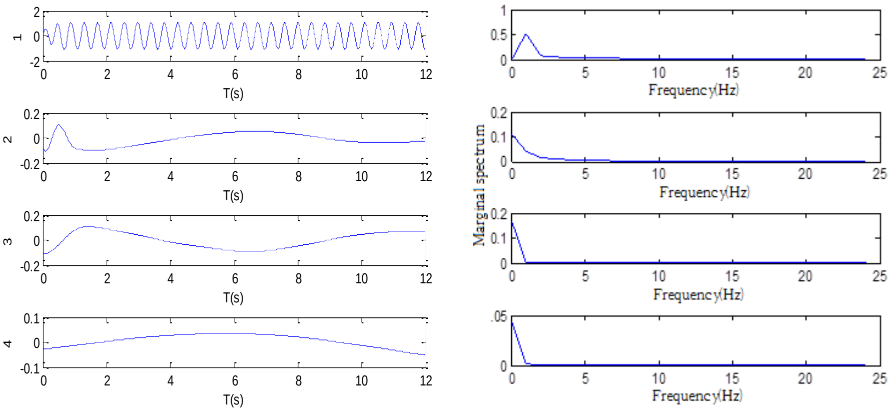

(a) IMFs of simulation signal *(b) corresponding frequency*

Fig. 8. Decomposition results of simulation signal at at rotating rate of 5rad/s.

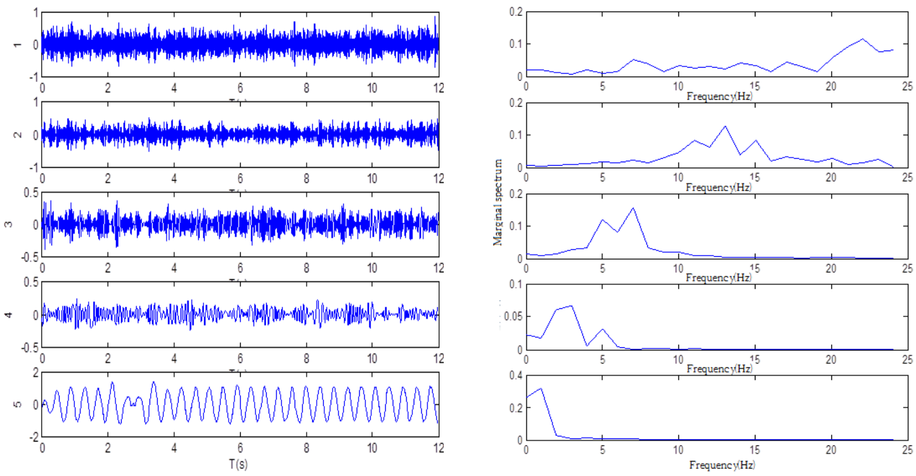

(a) the first IMF to fifth IMF *(b) corresponding frequency*

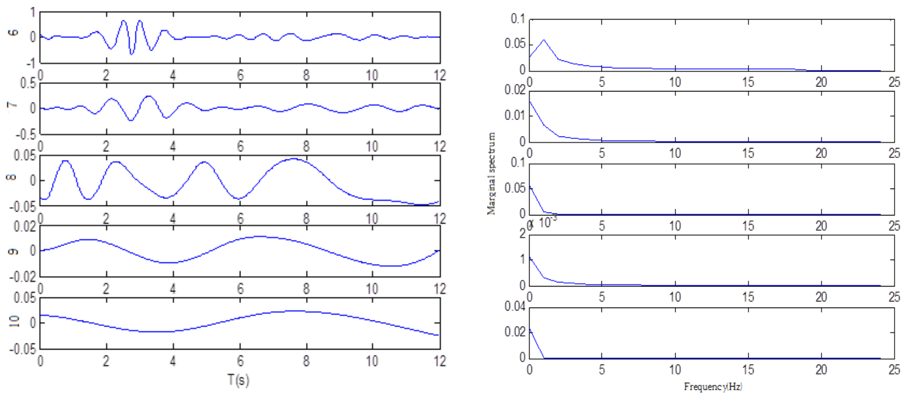

(c) the sixth IMF to tenth IMF *(d) corresponding frequency*

Fig. 9. Decomposition results of tested signal at at rotating rate of 5rad/s.

Table 1. The normalized energy of simulation signal and tested signal at rotating rate of 5rad/s.

IMF	Simulation signal	Tested signal	IMF	Simulation signal	Tested signal
1	0.84	0.11	6		0.07
2	0.05	0.06	7		0.02
3	0.07	0.04	8		0.01
4	0.03	0.07	9		0.03
5		0.58	10		0.01

Table 2. The normalized energy of simulation signal and tested signal at rotating rate of 12rad/s.

IMF	Simulation signal	Tested signal	IMF	Simulation signal	Tested signal
1	0.92	0.07	6		0.04
2	0.02	0.04	7		0.02
3	0.03	0.03	8		0.01
4	0.01	0.76	9		0.01
5	0.02	0.04			

Table 3. The normalized energy of simulation signal and tested signal at rotating rate of 30rad/s.

IMF	Simulation signal	Tested signal	IMF	Simulation signal	Tested signal
1	0.44	0.07	5	0.02	0.38
2	0.47	0.04	6	0.02	0.42
3	0.04	0.03	7		0.02
4	0.02	0.02	8		0.01

The tested signal and simulation signal at rotation rate of 12rad/s are decomposed into IMFs by the method of EMD , and then we calculate the normalized energy value of each IMFs by improved formula (8), and the results is shown in table 2. Table 2 shows the result of decomposition, the simulation signal is decomposed into five IMFs. And frequency of the first IMF is similar as the simulation signal which is concentrated in the rotating frequency, and the normalized energy of this IMF is 0.92, so this IMF is best represented the features of simulation signal, and physical meaning of this IMF is that the rotor motion is on state of periodic rubbing motion. Accordingly, the analysis results of tested signal are shown in Table 2. The signal is decomposed into 9 IMFs, and the frequency of each IMF has signification difference. Wherein, the frequency of fourth IMFs focuses on rotating frequency nearby, and the normalized energy is 0.76, so the this IMF is employed to represents the intrinsic physical meaning of measured signal, namely, because the effect of coupling faults on the rotor at higher rotation rate due to the rubbing phenomenon, the rotor running is in a periodic rubbing motion.

Table 3 shows the result of decomposition, the simulation signal at rotation rate of 30rad/s is decomposed into six IMFs. And frequency of the first IMF and second IMF are similar as the simulation signal which is concentrated in the rotating frequency and quarter to one-third rotating frequency, and the normalized energy of this IMF is 0.91, so this IMF is best represented the features of simulation signal, and physical meaning of this IMF is that the rotor motion is on state of chaotic motion. Accordingly, the analysis results of tested signal are shown in Table 3. The signal is decomposed into 8 IMFs, and the frequency of each IMF has signification difference. Wherein, the frequency of fifth IMFs and sixth IMFs focus on rotating frequency and quarter to one-third rotating frequency nearby, and the normalized energy is 0.74, so the this IMF is employed to represents the intrinsic physical meaning of measured signal, namely, because the effect of coupling faults on the rotor at higher rotation rate due to the rubbing phenomenon, the rotor running is in a chaotic motion.

5. Conclusions

This paper uses the EMD method which could be decomposed the intrinsic mode function according to the feature of signal to analyze the tested hydraulic generator rotor vibration signal at different rotation rate, the main conclusion are as followings:

(1) Comparing the frequency and normalized energy of IMFs which are acquired by EMD, the IMF which has main energy is represent the physical meaning and is closely related to the running state of rotor, namely, the IMF which has high frequency is represents the noise interference, and the IMF which has low frequency is represented the running trend of rotor, and the concentrated energy band IMFs which is called characteristic IMF is represents the rotor running type. When the frequency of characteristic IMF is concentrated in the rotating frequency, and the maximum value of IMF is less than 1mm, the rotor is in the state of stable periodic motion, otherwise, the rotor is in the state of periodic rubbing motion, when frequency of characteristic IMF is concentrated in the rotating frequency and quarter to one-third rotating frequency nearby, the rotor running is in a chaotic motion.

(2) The physical meaning of tested vibration signals could be captured by EMD method, which not only provides a new method for vibration signal analysis, but also lays the foundation for fault diagnosis of vibration signals.

Acknowledgments

This study is funded by the National Natural Science Foundation of China (No. 51179135).

References

[1] G. Song, Y. He, F. Chu et al, Expert Systems with Applications, **34**(1), 764 (2008).

[2] X. Xiang, J. Zhou, X. An, et al, Mechanical Systems and Signal Processing, **22**(7),1685 (2008).

[3] C. Ma, X. Gu, Y. Wang, Neurocomputing, **72**(13-15), 2909 (2009).

[4] M. Barakat, F. Druaux, D. Lefebvre, et al, Neurocomputing, **74**(18), 3865 (2011).

[5] Y. Papadopoulos, Reliability Engineering & System Safety, **81**(3), 325 (2003).

[6] N. Li, R. Zhou, Q. Hu, et al, Mechanical Systems and Signal Processing, **28**(0), 608 (2012).

[7] K. Thangavel, A. Pethalakshmi, Applied Soft Computing, **9**(1), 1 (2009).

[8] L. Jiamnin, L. Xiaolei, Z. Xiaoming, et al, Procedia Engineering, **16**(0), 224-229 (2011).

[9] Z. Xue, Y. Shang, A. Feng, Mathematics and Computers in Simulation, **80**(9), 1911 (2010).

[10] M. Feldman, Mechanical Systems and Signal Processing, **8**(2), 119 (1994).

[11] J. N. Yang, Y. Lei, S. Pan, N. Huang, Normal modes. EESD, **32**, 1443 (2003).

[12] B. L. Newkirk, H. D. Taylor, General Electric Review, **28**(8), 559 (1925).

[13] Cai-Wan Chang-Jian, Chao-Kuang Chen, Tribology International, **42**(3), 426 (2009).

[14] Cai-Wan Chang-Jian, Chao-Kuang Chen, Mechanism and Machine Theory, **42**(3), 312 (2007).

[15] Gwo-Chung Tsai, Journal of Sound and Vibration, **271**(3–5), 547 (2004).

*Corresponding author: hyqgxu@126.com